Electronic Supplementary Information

Design of hydrothermally-stable dawsonite-based sorbents in technical form for CO_2 capture

O. Martin, M. Hammes, S. Mitchell, and J. Pérez-Ramírez*

Institute for Chemical and Bioengineering, Department of Chemistry and Applied Biosciences, ETH Zurich, Vladimir-Prelog-Weg 1, CH-8093 Zurich, Switzerland

* Corresponding author. Fax: +41 44 633 1405; e-mail: jpr@chem.ethz.ch

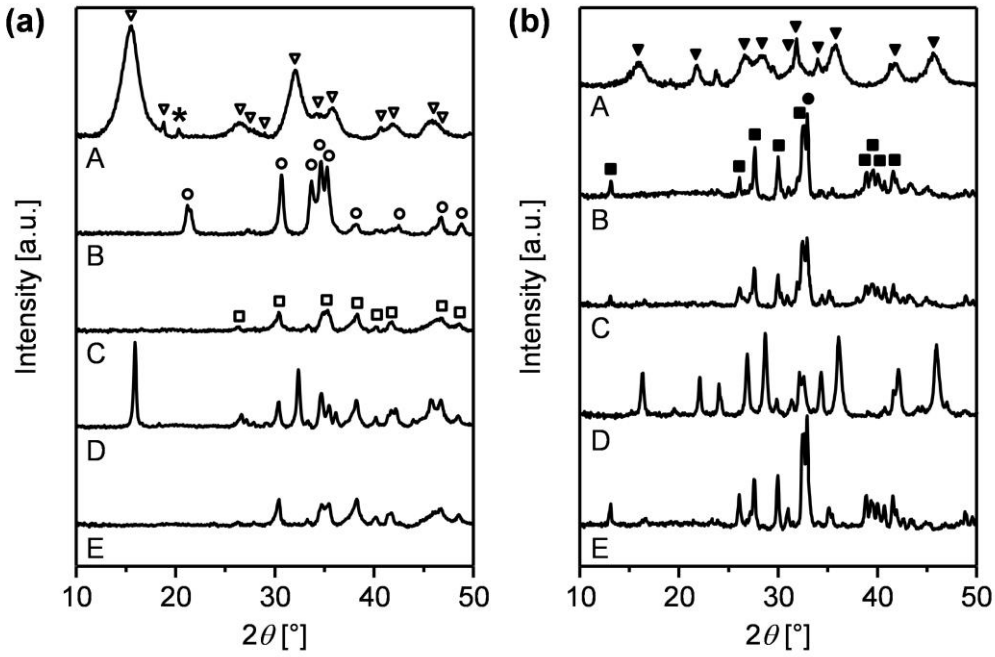

Fig. S1 XRD analysis of the evolution of the crystalline phases in (a) Na-dawsonite (Na-DW) and (b) K-dawsonite (K-DW): (A) as-synthesised, (B) fresh (calcined), (C) 1st regeneration, (D) 2nd carbonation, and (E) 2nd regeneration. Phase identification was achieved by comparison with the JCPDS reference patterns: (∇) $NaAlCO_3(OH)_2$ (83-1291), (□) Na_2CO_3 (86-287), (○) $NaAlO_2$ (83-316), (*) transition alumina, (▼) $KAlCO_3(OH)_2$ (21-979), (■) K_2CO_3 (71-1466), (●) $KAlO_2$ (89-8451), (★) $K_2(Al_2O(OH)_6)$ (76-455). Conditions of carbonation: 473 K, 3.0 MPa, $H_2O : CO_2 = 1 : 1$; regeneration: 773 K, 5 K min^{-1}, 3.0 MPa, Ar.

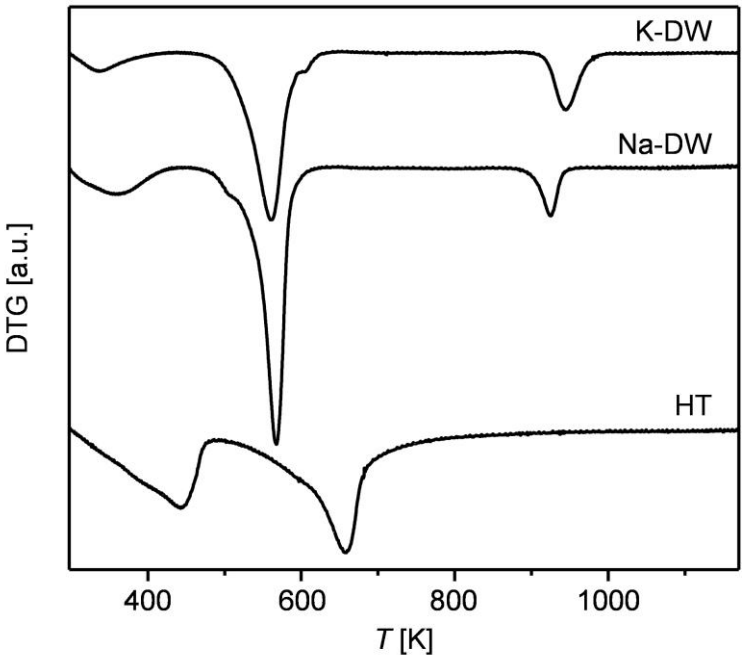

Fig. S2 First derivative of the weight loss curve of the as-synthesised K-DW, Na-DW, and hydrotalcite (HT) powders determined by thermogravimetric analysis. The measurements were undertaken in N_2 to simulate the inert atmosphere applied for sorbent regeneration. The peak observed at approximately 950 K in the dawsonite materials is consistent with the presence of alkali carbonates of high thermal stability, which are consequently not decomposed under the regeneration conditions used in this study (773 K). Furthermore, the bulk decomposition of the HT phase requires significantly higher temperatures (~100 K) compared with either of the dawsonites.

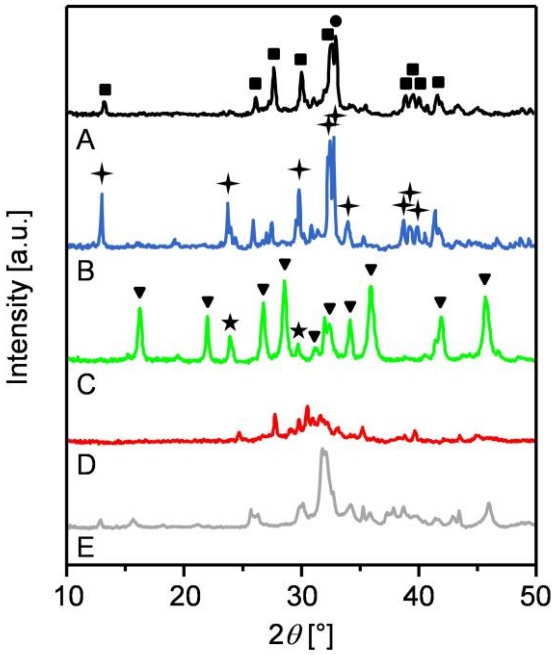

Fig. S3 XRD patterns of the K-DW powder sample isolated at different stages during the temperature-programmed sorption of CO_2 (Fig. 4b): (A) the fresh sorbent, (B) after bicarbonate formation at 303 K, (C) after dawsonite formation at 473 K, and (D) after decomposition at 673 K. Conditions: 0.1 MPa, $H_2O : CO_2 : N_2 = 5 : 5 : 90$, heating rate 5 K min^{-1}. Pattern (E) corresponds to the material isolated following decomposition of a single-phase K-DW powder at 773 K (5 K min^{-1}) and 3.0 MPa of CO_2 evidencing the potential to produce wet streams of carbon dioxide upon the regeneration of the sorbent. Principal crystalline phases were identified according to JCPDS reference patterns: (▼) $KAlCO_3(OH)_2$ (21-979), (★) $K_2(Al_2O(OH)_6)$ (76-455), (✦) $KHCO_3$ (70-1168), (●) $KAlO_2$ (89-8451), (■) K_2CO_3 (71-1466).

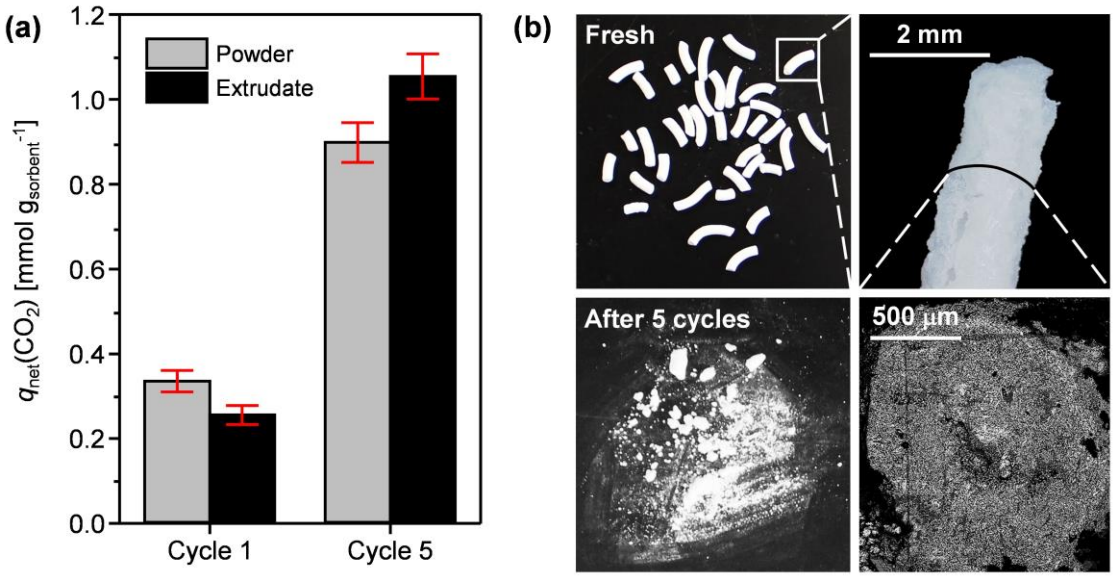

Fig. S4 (a) Net CO_2 capacity of the bulk K-dawsonite (K-DW) in powder and extrudate form in the 1st and 5th carbonation cycle. Reaction conditions as mentioned in Fig. S1. (b) Photographs of the bulk K-DW extrudates prior to the CO_2 capture experiment (top left) and after 5 cycles (bottom left). The optical micrograph (top right) shows the rough surface of a single body of fresh sample, while the SEM image of an internal cross-section (bottom right) highlights the dense structure. The loss in mechanical integrity of the extrudates upon the carbonation–regeneration cycles is attributed to the poor self-binding properties of the K-DW precursor.

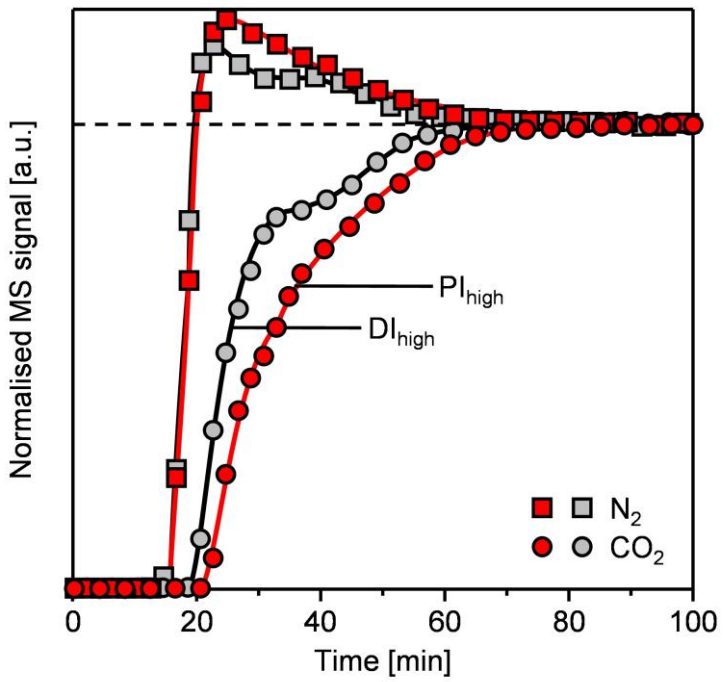

Fig. S5 Breakthrough curves in the 5th carbonation of the K_2CO_3/γ-Al_2O_3 extrudates prepared by dry- (DI_{high}) or paste-impregnation (PI_{high}). The enhanced carbonation kinetics observed over the former are related to the higher surface area, which is twice as high as the one displayed in the latter. Reaction conditions as detailed in Fig. S1.

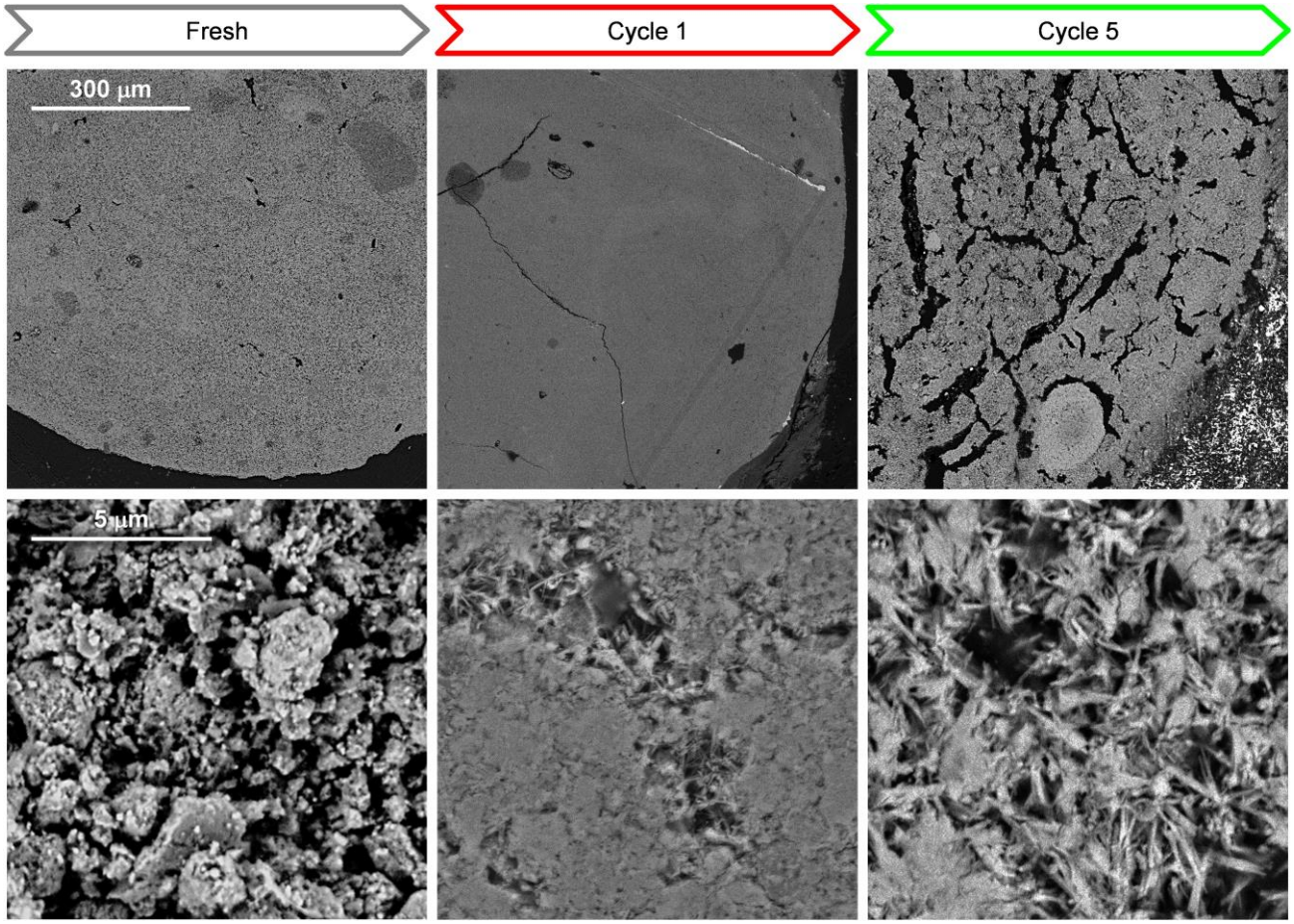

Fig. S6 SEM images of the dry-impregnated $K_2CO_3/\gamma\text{-}Al_2O_3$ sample (DI_{high}) at different magnifications in the fresh state, and after the 1st and 5th carbonation cycle. Crack formation induced by densification of the extrudate during the first carbonation cycle can be linked with the formation of needle-like dawsonite crystals, which continue to grow during consecutive carbonations while the sorbent equilibrates. The scale bar in the left micrograph applies to all images in the same row. See Fig. S1 for the reaction conditions applied.

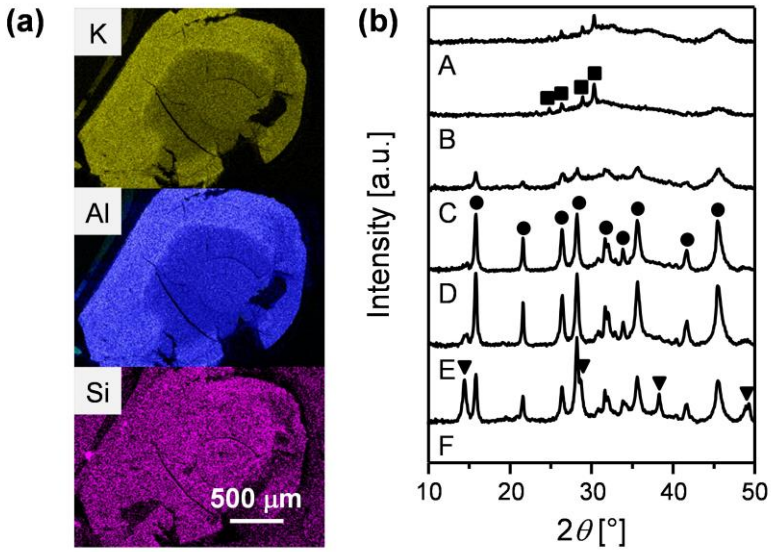

Fig. S7 (a) EDX mapping of the fresh DI_{high}-a sample revealing the egg-shell distribution of potassium in the attapulgite-bound alumina extrudates. No obvious concentration gradients of Si, which is present in the binder, were evidenced. (b) XRD patterns of the fresh K_2CO_3/γ-Al_2O_3 extrudates prepared by dry impregnation; (A) additive-free (DI_{high}), (B) with 10 wt% starch (DI_{high}-s), and (C) prepared with 10 wt% attapulgite (DI_{high}-a). Corresponding analysis of the samples after the 5th carbonation cycle is depicted in the patterns (D), (E), and (F), respectively. Crystalline phases indicated were identified according to JCPDS reference patterns: (●) $KAlCO_3(OH)_2$ (21-979), (■) K_2CO_3 (71-1466), (▼) AlO(OH) (74-2895). Reaction conditions as specified in Fig. S1.